


Magnetic Targeting of Stem Cell Derivatives Enhances Hepatic Engraftment into Structurally Normal Liver

Cell Transplantation
2017, Vol. 26(12) 1868–1877
© The Author(s) 2018
Reprints and permission:
sagepub.com/journalsPermissions.nav
DOI: 10.1177/0963689717737320
journals.sagepub.com/home/cil


W. Samuel Fagg^{1,2}, Naiyou Liu^{1,2}, Ming-Jim Yang³, Ke Cheng⁴,
Eric Chung⁴, Jae-Sung Kim⁴, Gordon Wu⁵, and Jeffrey Fair^{1,2}

Abstract

Attaining consistent robust engraftment in the structurally normal liver is an obstacle for cellular transplantation. Most experimental approaches to increase transplanted cells' engraftment involve recipient-centered deleterious methods such as partial hepatectomy or irradiation which may be unsuitable in the clinic. Here, we present a cell-based strategy that increases engraftment into the structurally normal liver using a combination of magnetic targeting and proliferative endoderm progenitor (EPs) cells. Magnetic labeling has little effect on cell viability and differentiation, but in the presence of magnetic targeting, it increases the initial dwell time of transplanted EPs into the undamaged liver parenchyma. Consequently, greater cell retention in the liver is observed concomitantly with fewer transplanted cells in the lungs. These highly proliferative cells then significantly increase their biomass over time in the liver parenchyma, approaching nearly 4% of total liver cells 30 d after transplant. Therefore, the cell-based mechanisms of increased initial dwell time through magnetic targeting combined with high rate of proliferation in situ yield significant engraftment in the undamaged liver.

Keywords

magnetic targeting, stem cell, engraftment, quiescent liver

Introduction

Cell transplantation may be a viable alternative to orthotopic liver transplantation for the treatment of liver-based inborn errors of metabolism.^{1,2} However, there are few reports (pre-clinical or otherwise) of long-term engraftment and repopulation of the recipient organ with transplanted cells without preconditioning liver injury. In patients severely affected by urea cycle defects, such as neonatal onset of *Ornithine transcarbamylase (OTC)* deficiency, hepatocyte transplantation can provide a short-term therapeutic effect, but recipients require either repeated doses of transplanted hepatocytes or ultimately liver transplant^{3,4} presumably due to the low proliferative capacity and high turnover rate of transplanted hepatocytes. Thus, hepatocyte transplantation can be an effective strategy to delay organ transplant in urea cycle defect patients but fails to provide a long-term solution.

Experimental methods to increase liver engraftment efficiency of a variety of transplanted cell types in rodent models require extensive parenchymal injury to the recipient liver,^{5–7} and these methods are not easily translated to the clinical setting.⁸ Clinical methods of increasing engraftment include irradiation or portal vein embolization,^{8,9} which still

involve risk to the recipient including morbidity.^{10–12} Therefore, a cell transplantation-based strategy that can be used in the clinic (i.e., does not require liver injury in the recipient) and results in long-term persistence of transplanted cells would increase patient quality of life and reduce the demand for liver transplant.

¹ Transplant Division, Department of Surgery, University of Texas Medical Branch Galveston, TX, USA

² Shriners Hospital for Children, University of Texas Medical Branch, Galveston, TX, USA

³ Department of Surgery, University of Florida, Gainesville, FL, USA

⁴ Department of Medicine, Cedars-Sinai Medical Center, Los Angeles, CA, USA

⁵ Comprehensive Transplant Center, Cedars-Sinai Medical Center, Los Angeles, CA, USA

Submitted: April 12, 2017. Revised: August 23, 2017. Accepted: September 01, 2017.

Corresponding Author:

Jeffrey Fair, Transplant Division, Department of Surgery, University of Texas Medical Branch, John Sealy Annex 6.206, 301 University Boulevard, Galveston, TX 77550, USA.

Email: jhfair@utmb.edu



Creative Commons CC BY-NC: This article is distributed under the terms of the Creative Commons Attribution-NonCommercial 4.0 License (<http://www.creativecommons.org/licenses/by-nc/4.0/>) which permits non-commercial use, reproduction and distribution of the work without further permission provided the original work is attributed as specified on the SAGE and Open Access pages (<https://us.sagepub.com/en-us/nam/open-access-at-sage>).

Transplantation of partially differentiated stem cells may provide a long-term solution for repopulation of the quiescent liver independent of liver damage. We have shown that endoderm progenitor (EP) cells, which are early derivatives of embryonic stem cells, engraft into the quiescent liver without preconditioning damage and reverse the phenotype of a mouse model of hemophilia B.¹³ Although effective, the observed engraftment was quantitatively inconsistent, leading us to test both *in vitro* and *in vivo* strategies to standardize engraftment and increase its efficiency. In this study, we find that using a more proliferative EP cell, combined with magnetic targeting to the liver, increases the efficiency and reproducibility of engraftment in the quiescent liver independent of preconditioning damage. These findings together with our previous studies¹³ suggest the use of EP cells and magnetic targeting may provide a long-term strategy to reduce disease phenotype of liver-based inborn errors of metabolism.

Materials and Methods

Mouse ES Cell Culture and Differentiation

The ES cells used are derived from strain 129P2_Ola mice and constitutively expresses green fluorescent protein (GFP) driven by the β -actin promoter.^{13,14} Cells were maintained on murine embryonic fibroblast feeder layers that produce leukemia inhibitory factor. Embryonic stem cell (ESC) propagation media was high glucose Dulbecco's modified Eagle's medium (DMEM) (Sigma, USA) supplemented with 15% Fetal Bovine Serum (FBS) (Sigma), 0.1 mM 2-mercaptoethanol (Sigma), 100 units/mL penicillin, and 100 g/mL streptomycin (GIBCO, USA).¹³ To ensure viability and pluripotency, ESC media were changed daily, and cells were passed every 2 to 3 d. Cells were passed using trypsin (0.05% trypsin, in 0.53 mM ethylenediaminetetraacetic acid [EDTA]) for 3 min followed by filtration through a 40- μ m strainer to remove differentiated cells. After at least 2 passages from frozen stocks, the cells were used for experiments.

Two different methods were used for endoderm induction: (1) mouse ES cells were plated at 4×10^5 cells/collagen-coated 35 mm² dish and grown in ESC propagation media supplemented with 100 ng/mL acidic fibroblast growth factor (FGF) (Sigma) for 5 to 7 d as described¹³ or (2) embryoid bodies were collected after 2.5 d then subjected to a 2-step protocol using serum-replacement media supplemented with 100 ng/mL human activin A (R&D Systems, USA) as described.¹⁵ Trypan blue exclusion for cell viability was performed as described,¹⁶ and growth curves were assessed by trypan blue excluding cells counted in both technical and biological triplicate during the differentiation time course and used to calculate doubling times. The BrdU/7AAD staining assay was performed as described by the manufacturer (BD Pharmingen, USA). Hepatic differentiation was induced using day 8 endoderm cells (from acidic FGF method, see above) incubated in Hepatocyte

Culture Media (HCM, Lonza, USA) supplemented with 30 ng/mL FGF4 (R&D Systems, Minneapolis, USA) and 20 ng/mL bone morphogenetic protein 2 (BMP2) (R&D Systems) for 2 d, followed by 4 d in HCM supplemented with 20 ng/mL hepatic growth factor (HGF) (R&D Systems), 10 ng/mL oncostatin M (R&D Systems), and 0.1 μ M dexamethasone (R&D Systems).

Superparamagnetic Microsphere (SPM) Labeling of EP Cells

EPs were labeled with fluorescent (flash red) SPM particles (0.9 μ m diameter; Bangs Laboratories, Fishers, IN, USA) by incubation in cell culture for 24 h. Successful labeling was confirmed by flash-red fluorescence. Labeling efficiency was assessed by flow cytometry. *In vitro* toxicity experiments were performed 24 h after SPM labeling. Cell viability was assessed by trypan blue exclusion. Apoptosis and necrosis were assessed by flow cytometry using 7AAD and annexin-V stains (BD Pharmingen, San Jose, CA, USA). Albumin (Alb) and α -fetoprotein messenger RNA (mRNA) abundance were measured by quantitative real-time polymerase chain reaction (PCR) (see below).

Animals

Wild-type Balb/c mice were obtained from Jackson Laboratory and housed in the Animal Care Services Facility at the University of Florida. All mice weighed from 15 to 25 g. Mice were maintained on standard chow and kept on a 12-h light/dark cycle. All procedures performed were approved by the Institutional Animal Care and Usage Committee at their respective institutions and thus in compliance with the guidelines for humane care of laboratory animals.

Transplantation of EP Cells

EPs (1×10^6) were suspended in phosphate buffered saline (PBS) with 1% fetal bovine serum (FBS) and 0.1 mM ethylenediaminetetraacetic acid (EDTA) and incubated on ice for no more than 30 min while awaiting transplant. Mice were anesthetized with an intraperitoneal (IP) injection of ketamine and dexmedetomidine or inhaled isoflurane. A small incision was created either below the right costal margin or along the midline. The cell suspension was injected into the portal vein using a 30-G needle with a magnet in place on the adjacent body wall. Atipamezole (1.0 mg/kg, IP) was used to reverse anesthesia if ketamine were used. Mice were dosed with 0.1 g/kg IP buprenorphine after surgery and monitored closely thereafter. Following skin wound closure, a 1.3 Tesla magnet (K&J Magnetics, Inc.) sheet (15 \times 15 \times 2 mm³) was attached to the skin with a bandage at the right lower rib cage and was kept in place for 18 h.

Hepatocyte Isolation and Fluorescence Activated Sorting of GFP Positive Cells

Hepatocytes were isolated from mouse livers after EP + SPM injection by a sequential perfusion method as previously described.¹⁷ Briefly, the inferior vena cava was cannulated with an 18 G intravenous (IV) catheter. The portal vein was severed and the suprahepatic vena cava was tied off. The liver was then perfused first with an EGTA solution, followed by collagenase at 100 collagen digestion units (CDU/mL). The resulting cell suspension had greater than 80% viability as measured by the trypan blue exclusion assay and was then analyzed and sorted using a FACSAria II flow cytometer (BD Biosciences) equipped with a combination of 407, 488, 561, and 640 nm lasers. Sorted cells were deflected into Falcon tubes containing PBS + 20% fetal calf serum.

Quantitative RT-PCR

Real-time fluorescent quantitative PCR was performed as described previously.¹³ Briefly, total RNA was harvested and purified using the RNeasy Mini Kit (Qiagen). One microgram was reverse transcribed using the QuantiTect Reverse Transcription Kit (Qiagen) following the manufacturer's directions. The resultant cDNA template was diluted 50-fold and 100 pg of template amplified in RT2 SYBR Green/ROX qPCR Master Mix (SABiosciences-Qiagen) on an ABI 7300 optical thermocycler (Applied Biosystems). For each amplification, a no template control was performed to ensure no detectable product was formed from spurious primer-only amplification. Relative levels of mRNA were normalized to β -actin, which was used as the internal control. The primer sequences were used for β -actin (forward: 5'-ATGCTCCCCGGGCTGTAT-3', reverse: 5'-CATAGGAGTCCTTCTGACCCATTC-3'), α -fetaprotein (Afp; forward: 5'-ATTGCCTCCACGTGCTGCCA-3', reverse: 5'-GAAAATGTGCGCCATTCCT-3'), Alb (forward: 5'-GGCACCAAGTGTGTACACT-3', reverse: 5'-AGCAGACACACACGGTTCAG-3'), hepatocyte nuclear factor 4 alpha (Hnf4a; forward: 5'-ACACGTCCCCATCTG AAG-3', reverse: 5'-CTTCCTTCTTCATGCCAG-3'), Cyp3a (forward: 5'-TGGGTGAGTGGT TGCTTACA-3', reverse: 5'-GAGG-GAAACTGGTGAGGATG-3'), transferrin (forward: 5'-GGTCCCTCGAAAGATAGACATCA-3', reverse: 5'-GGGAGTCTTCAGACCTC TTTTAA-3'), and α -1-antitrypsin (a-1-AT; forward: 5'-AATGGAAGAAGCCATTC-GAT-3', reverse: 5'-AAGACTGTAGCTGCTGCAGC-3').

3-D Microscopy

Fresh liver explants were examined with a stereomicroscope (MZ16FA, Leica Microsystems) using a GFP2 long-pass filter (100447084, Leica Microsystems) to detect the presence of GFP-positive cells.

Statistical Analysis

Results are presented as mean \pm standard deviation from 3 independent biological replicates unless specified otherwise. Comparisons between 2 groups were performed using 2-tailed unpaired Student's *t*-test, and comparisons consisting of more than 2 groups were performed using two-way analysis of variance. Differences were considered statistically significant when $P \leq 0.05$ and are noted as such where applicable.

Results

Cell Proliferation Rate Correlates with Engraftment in Quiescent Liver

Initially, the aim of this study was to compare different endoderm differentiation methods for differentiation efficiency, cell proliferation, and viability rates and correlate these with engraftment efficiency in undamaged mouse liver. We hypothesized a more efficiently differentiated EP cell population that was highly proliferative and viable would engraft more readily in the quiescent liver. We previously measured markers of endoderm (Sox17, FoxA2, and Gata4), mesoderm (Nkx2.5, gooseoid), ectoderm (nestin, Pax6), pluripotent (Oct4), and hepatic (Afp, Alb) gene expression in acidic fibroblast growth factor (aFGF) differentiation time courses and find efficient induction of endoderm transcripts and proteins, but low to undetectable levels of other lineage marker mRNAs.^{13,14,18,19} Comparing these results to those obtained using the ActivinA differentiation method¹⁵ indicated induction of various endoderm marker mRNAs and that pluripotency-related transcripts are also reduced using each differentiation protocol.^{15,18,19} Additionally, we detected very few dead cells during both the aFGF and ActivinA 6-d differentiation time course (Fig. 1A and data not shown), indicating no significant difference in cell viability between the 2 methods. Therefore, we conclude these 2 differentiation methods yield efficiently differentiated EP cell populations with a low level of cell death.

In contrast, we observe a striking difference in the proliferation rate of EPs produced from these 2 different endoderm differentiation protocols: EP cells produced from the aFGF (aFGF-EPs) method have a significantly higher proliferation rate (doubling time of 19.5 h) compared to cells from the ActivinA method (activin-EPs) with doubling time of 28.7 h (Fig. 1A; $P \leq 0.01$). A complementary approach supports this finding, as a significantly greater percentage of aFGF-EP cells are in S phase of the cell cycle (Fig. 1B; $P \leq 0.01$) as determined by BrdU/7AAD staining and flow cytometry analysis. Therefore, aFGF-EPs and activin-EPs have similar endoderm and pluripotency marker gene expression profiles and levels of cell viability, but aFGF-EPs proliferate at a significantly higher rate. We next tested the liver engraftment efficiency of EPs by portal vein injection in Balb/c mice and analysis of whole liver explant using fluorescent stereomicroscopy,²⁰ which allows us to detect GFP+

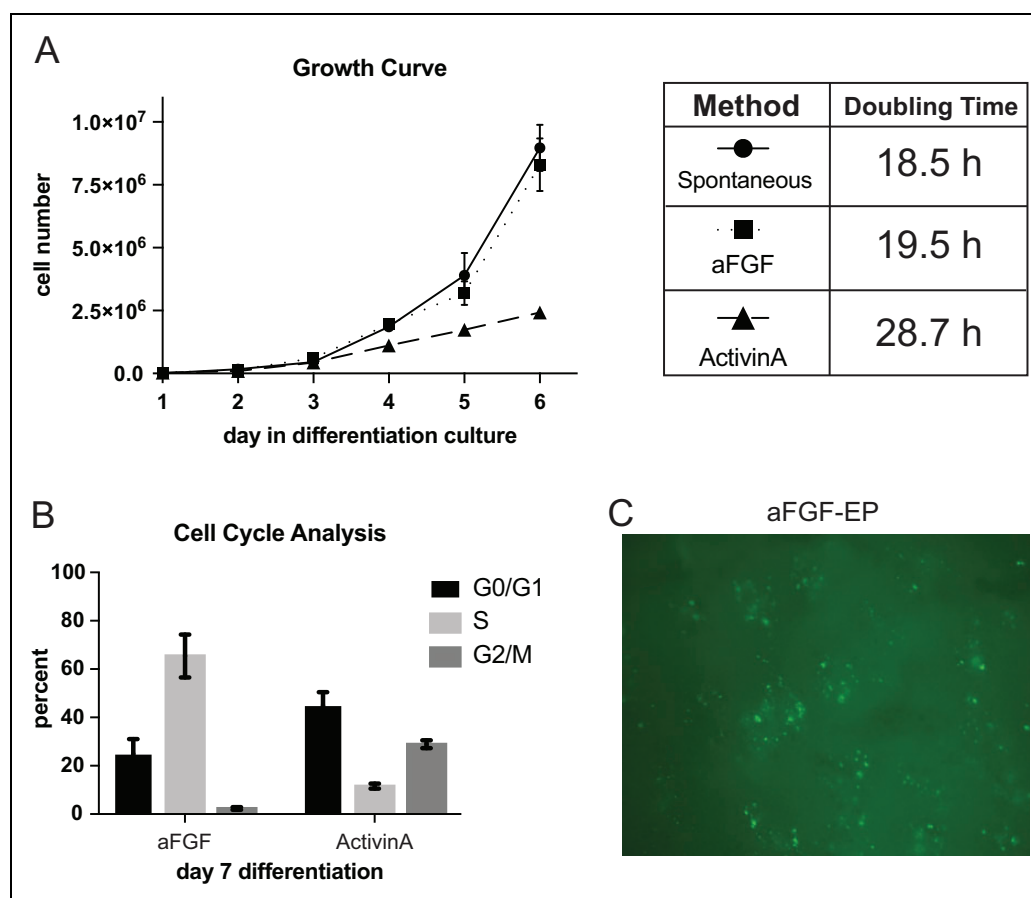


Fig. 1. High proliferation rate positively correlates with endoderm progenitor (EP) cell liver engraftment. (A) Trypan blue exclusion assay was performed on spontaneously differentiated ES cells or ES cells undergoing the aFGF or Activin A methods for 6 d to generate growth curves. Average cell numbers for each day were recorded from biological triplicate cultures (error bars represent standard deviation [SD] from the mean) and used to calculate doubling time for each culture condition. (B) BrdU/7AAD staining was performed on day 7 differentiated aFGF-EPs and Activin-EPs and analyzed by flow cytometry to determine cell cycle phase distribution of biological triplicate cultures with error bars representing SD from the mean. (C) Representative image of whole liver analyzed by stereomicroscopy using fluorescein isothiocyanate (FITC) filter to identify green fluorescent protein-positive cells 14 d after aFGF-EP transplant ($10\times$ magnification).

cells several millimeters deep within the organ (see online Fig. S1 for experimental overview). Fourteen days after transplant of aFGF-EPs and activin-EPs, we readily detected transplanted GFP-positive aFGF-EP cells in liver explants (Fig. 1C and consistent with our previous observations¹³) but were unable to detect GFP-positive activin-EP cells under the same conditions ($N = 3$ each). These findings support the conclusion that a more proliferative EP cell may be a superior engraftment candidate for delivery to the undamaged liver parenchyma.

SPM-labeled EP Cells Maintain Viability and In Vitro Differentiation Capacity

Based on the above results, we focused on using the aFGF-EP and reasoned that enhancing early transplant events such as cell delivery and initial dwell time in the liver (independent of preconditioning injury) would further contribute to engraftment efficiency of aFGF-EPs. Magnetic targeting

using cells labeled with superparamagnetic (SPM) nanoparticles increases engraftment into disparate target tissues,^{21–24} therefore this approach may further increase engraftment of aFGF-EPs in the undamaged liver. This process involves the endocytosis of iron particles (SPMs) by cells of interest, which can then be attracted and retained by a magnetic field.²⁵ Because of iron's potential toxicity, we first tested whether internalization of SPMs affected cell viability or differentiation.

aFGF-EPs were differentiated for 6 d then incubated with SPMs conjugated to flash-red fluorophore at a ratio of 500:1; 1,000:1; and 2,000:1 (SPM:cell) for 24 h to determine optimal dosage for cell labeling and potential toxicity of SPM incorporation into EP cells. We confirmed particle uptake by aFGF-EPs that constitutively express GFP using both confocal microscopy (Fig. 2A) and flow cytometry (Fig. 2B). The average percentage of SPM-labeled cells after 24 h is $83.6\% \pm 3.1$ (Fig. 2C), indicating label saturation at a ratio of 500:1, as no increase in cell labeling is

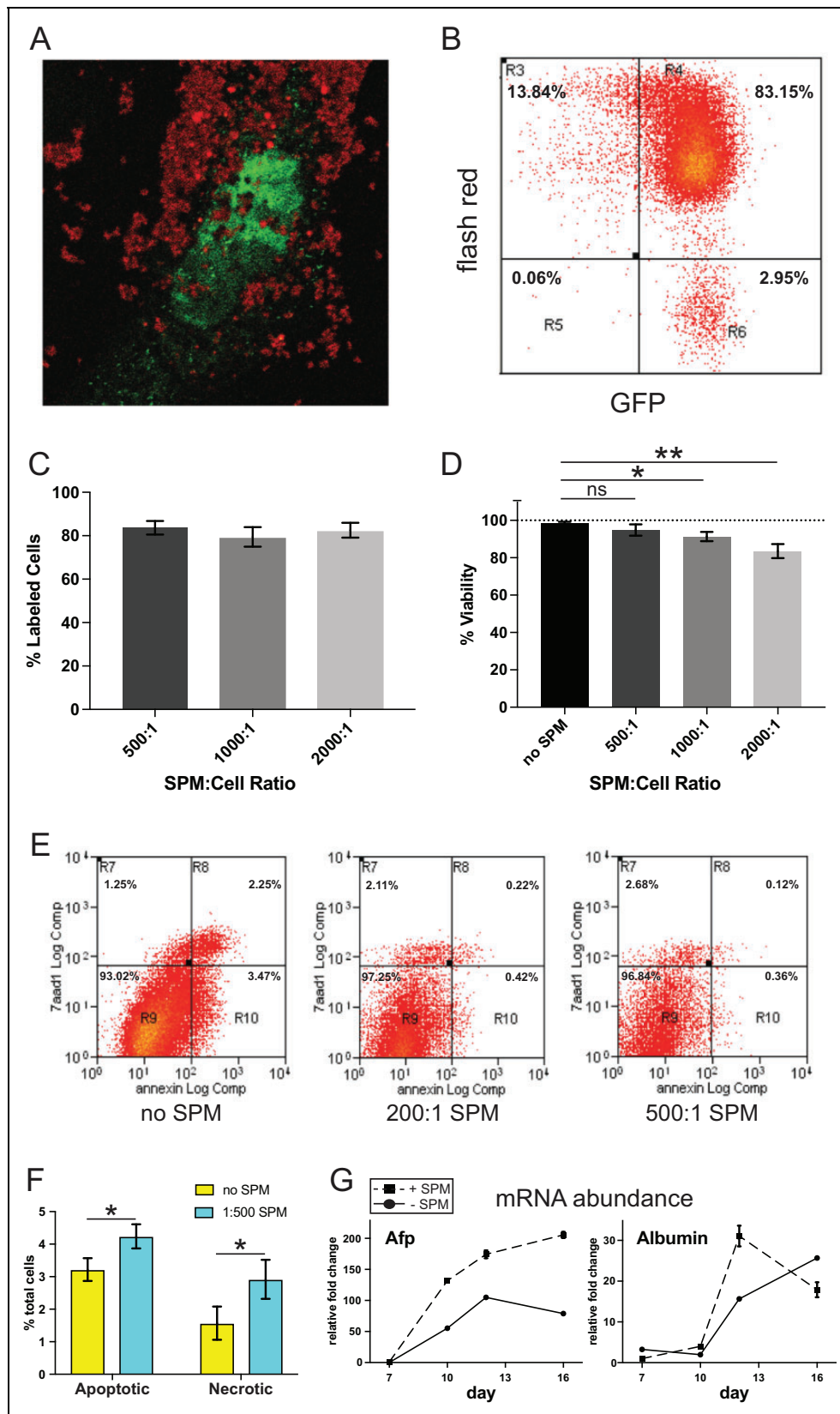


Fig. 2. Superparamagnetic microsphere (SPM) labeling does not deleteriously affect aFGF-endoderm progenitor (EP) viability or hepatic lineage progression. (A) Day 7 differentiated aFGF-EP cells were incubated with flash-red fluorescent chromosome labeled SPMs for 24 h and analyzed by confocal microscopy at 60 \times magnification; image shows a single cell with nuclear-localized green fluorescent protein. (B) aFGF-EP cells were labeled with SPMs as in (A) and analyzed by flow cytometry. (C) Day 7 differentiated aFGF-EP cells were incubated with

detectable at higher ratios (Fig. 2C). Using the trypan blue exclusion assay, we observe no significant change in cell viability at the 500:1 (SPM:cell) ratio; however, both the 1,000:1 and 2,000:1 ratios are correlated with significant increases in cell death (Fig. 2D; $P \leq 0.05$ and $P \leq 0.01$, respectively). However, measurement using the more sensitive annexin-V/7-AAD assay (Fig. 2E) indicates a statistically significant, but nominal, increase in apoptotic and necrotic cells of 1% each using the 500:1 ratio (Fig. 2F). Therefore, a ratio of 500:1 efficiently labels aFGF-EPs without adversely affecting cell viability and causes them to be attracted and retained by a magnetic field in vitro (online Fig. S2).

To test if SPM labeling disrupts the differentiation process, day 6 aFGF-EPs were labeled with SPMs as above, then differentiated toward the hepatic lineage, and markers for hepatoblast (Afp) and hepatocyte (Alb) formation were measured 1, 3, 5, and 10 d post-SPM labeling. Measurement of Afp and Alb mRNAs shows comparable induction over the differentiation time course between cells incubated with and without SPM (Fig. 2G). This indicates the in vitro differentiation potential of these cells to form hepatoblast- and hepatocyte-like cells is not compromised by SPM labeling. In summary, SPM labeling aFGF-EPs neither drastically alters cell viability nor interrupts the hepatic differentiation program in vitro; therefore, SPMs may be a suitable tool to boost in vivo liver engraftment independent of liver injury.

Magnetic Targeting Increases aFGF-EP Engraftment Efficiency in Undamaged Liver

SPM labeling aFGF-EP cells followed by magnetic targeting may be an effective method to increase the initial dwell time of transplanted cells to recipient undamaged liver parenchyma. Accordingly, we hypothesize an increase in dwell time combined with a proliferative transplanted cell may be sufficient to achieve quantitatively significant engraftment independent of preconditioning liver damage. To test if magnetic targeting can increase liver engraftment of FGF-EPs in vivo, we injected SPM-labeled GFP-positive aFGF-EPs into the portal vein of wild-type Balb/c mice with or without a 1.3 Tesla magnet applied to the outer body wall during and 18 h postinjection and monitored engraftment efficiency. Initial engraftment rates drop dramatically after 48 h,²⁶ so the presence of GFP-positive cells

from collagenase-digested recipient livers was assessed at multiple time points: 30 min, then 1, 3, 7, and 30 d post-transplant by flow cytometry. Consistent with enhancement of the initial dwell time in the liver, we observe a significant increase in percentage of GFP-positive cells 30 min posttransplant using magnetic targeting (Fig. 3A). In fact, at each time point analyzed, there is a significantly higher percentage of GFP-positive cells when using magnetic targeting enhanced aFGF-EP transplant compared to control transplants without magnetic targeting (Fig. 3A). Consistent with previous results,²⁶ we also observe an initial and steady decline in GFP-positive cell numbers in situ (30 min to 3 d); however, the significant increase between 7 and 30 d (Fig. 3A) suggests a period of exponential cell growth in vivo. Additionally, qualitative analysis of engraftment in fresh frozen tissue sections of livers at 30 d posttransplant shows readily detectable fluorescent clusters of cells, similar to previous observation,¹³ but more robust clusters are detected with magnetic targeting (Fig. 3B). We conclude that magnetic targeting significantly increases aFGF-EP engraftment efficiency in the undamaged liver, in part by increasing the initial dwell time within the parenchyma.

To determine whether magnetic targeting has any adverse effect on terminal differentiation of aFGF-EPs in vivo, GFP-positive cells were retrieved from mouse livers 30 d posttransplant by fluorescence activated cell sorting (FACS) (Fig. 3C), and mRNA abundance was measured for liver-specific mRNA expression (Fig. 3D). We compared mRNA abundance from transplanted GFP+ cells retrieved from the liver after 30 d, along with native mouse hepatocytes (positive control), day 7 differentiated aFGF-EPs (undifferentiated control pretransplant), and spleen (negative control) by RT-qPCR for the liver-specific mRNAs Alb, HNF4A, Cyp3a, transferrin, and $\alpha 1$ antitrypsin. The results indicate the engrafted GFP+ cells have a very similar gene expression profile to hepatocytes (Fig. 3D), thus SPM-labeled EPs engraft then differentiate to hepatocyte-like cells in vivo.

Since magnetic targeting appears to promote retention of aFGF-EPs in the liver parenchyma immediately and up to 1 wk after transplant (Fig. 3A), we hypothesized this strategy might inhibit vascular flow-through of transplanted cells into the lungs. If so, the transplanted cells would indeed have enhanced dwell time within the liver, which would aid engraftment within the parenchyma and subsequent proliferation in situ. A potential unintended consequence of this,

Fig. 2. (continued). ratios of 500:1; 1,000:1; and 2,000:1 SPM:cells for 24 h, and labeling efficiency was measured by flow cytometry; data shown are average of 3 independent biological replicates with standard deviation (SD) of the mean shown with error bars. (D) Cell viability was measured by trypan blue exclusion assay after SPM labeling as in (C); * $P < 0.05$ and ** $P < 0.01$ by two-way analysis of variance with Dunnett's multiple comparisons test. (E) Day 7 aFGF-EPs were mock labeled or incubated with 200:1 or 500:1 SPM for 24 h, then stained using annexin-V/7AAD and measured by flow cytometry (representative images from biological triplicate cultures shown). (F) Quantitative summary of results for no SPM and 500:1 SPM labeled day 7 aFGF-EPs as measured in (E); data shown are the average obtained from biological triplicates with SD shown with error bars; * $P < 0.05$ by student's t-test. (G) Day 7 aFGF-EPs were mock labeled or labeled at a 500:1 ratio with SPM and subjected to further differentiation along the hepatic lineage (see Materials and Methods section for details), and RNA was collected at days 7, 10, 12, and 16 to measure abundance of α -fetoprotein and albumin mRNA relative to β -actin by RT-qPCR; mean relative fold change shown compared to baseline value determined at day 7 from cells cultured in biological triplicate with error bars denoting SD.

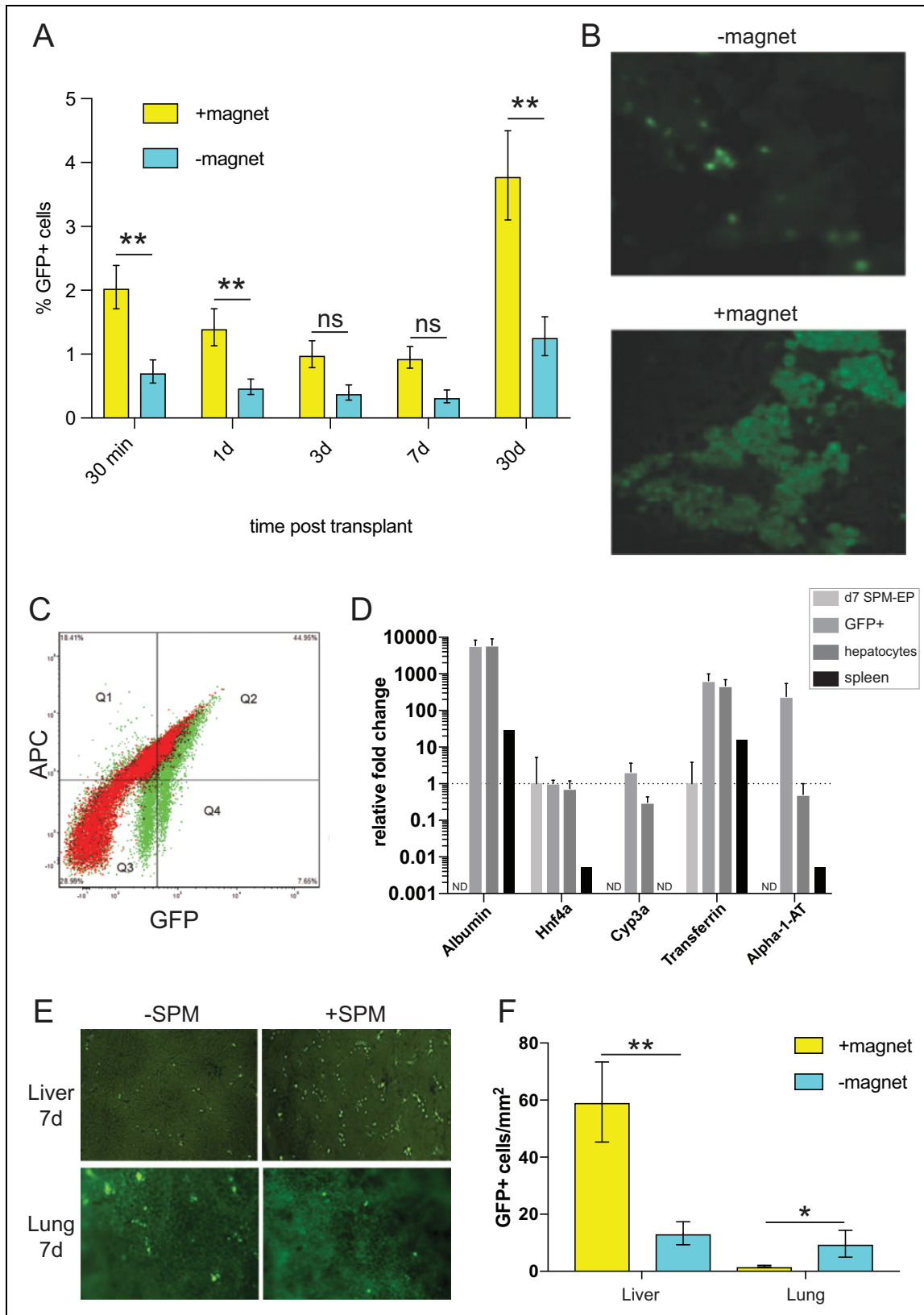


Fig. 3. Magnetic targeting increases liver engraftment efficiency of aFGF-endoderm progenitors (EPs). (A) Day 7 differentiated green fluorescent protein (GFP)+ aFGF-EPs were incubated with superparamagnetic microspheres (SPMs) at a 1:500 ratio for 24 h and injected into mouse portal vein with (+magnet) or without (-magnet) magnets fixed on the outer body wall. Engraftment was assessed at 0.5 h, 1, 3, 7, and 30 d after transplantation by identification of GFP+ cells from livers perfused to a single-cell suspension determined by flow cytometry

though, is magnetic field-enhanced dwell time/retention could lead to cell clumping resulting elevated stasis and subsequent thrombosis, as has been reported in hepatocyte transplantation.²⁷ To address this possibility, we examined the transplanted cells' localization patterns within the sinusoid of livers very early during the engraftment process, as cell clumping/cohesion will be readily apparent if it is a major consequence of magnetic targeting. Stereomicroscopy of liver explant 30 min after delivery of SPM-EPs shows GFP+ cells distributed diffusely and stochastically throughout the sinusoid. However, 24 h posttransplant a characteristic pattern of localization around the periphery of the sinusoid is evident for aFGF-EPs, independent of magnetic targeting (online Fig. S3; $N = 3$ each), which is consistent with localization patterns observed at later time points (online Fig. S1 [4 d] and also see Fig. 3E [7 d]), suggesting that occlusion of the portal vessels does not contribute to magnetic targeting-based enhancement of engraftment. Furthermore, we determined the number of GFP+ cells per area of microscopic field of view (Fig. 3E) in both the liver and the lungs of mice receiving transplanted aFGF-EPs with or without magnetic targeting 7 d posttransplant. Delivery enhanced with magnetic targeting results in significantly fewer GFP+ cells in the lung ($P \leq 0.05$) and more GFP+ cells in the liver ($P \leq 0.01$) per square millimeter area than without magnetic targeting (Fig. 3F). Taken together, these results indicate magnetic targeting aFGF-EPs increases overall dwell time of aFGF-EP cells in the liver, significantly increasing the quantitative engraftment of these cells in the undamaged liver parenchyma without the development of portal occlusion and thrombosis.

Discussion

We present here a strategy that can be rapidly adopted in the clinic to increase the initial engraftment of transplanted cells into the quiescent, undamaged liver parenchyma. Previous studies utilizing hepatocyte transplantation have required parenchymal damage, that is, hepatectomy or retrorsine, for significant engraftment to occur.^{7,8,28,29} Even then, multiple injections may be necessary to attain a therapeutic effect.^{26,30} Justifying these strategies for patients with

metabolic alterations but otherwise normal livers may be difficult; indeed, hepatocyte transplantation in *OTC* deficient patients only provides a short-term benefit while awaiting liver transplant.^{3,4,31} Furthermore, the relatively large size of hepatocytes at $\sim 40 \mu\text{m}$ and a report of portal thrombosis in a hepatocyte transplant recipient²⁷ presents additional challenges. Our cell transplant strategy combining magnetic targeting with proliferative, relatively small EPs ($\sim 20 \mu\text{m}$ ^{18,19}) provides a novel proof-of-concept that long-term, quantitatively significant engraftment can be achieved in the undamaged mouse liver. These findings along with our previous study indicate aFGF-EP cells can differentiate and function as hepatocytes *in vivo*, as they are able to produce factor IX and reverse a hemophilic phenotype.¹³

The striking difference in proliferation between the aFGF-EP and activin-EP cells derived from identical mouse ES cell cultures positively correlates with liver engraftment 2 wk posttransplant (Fig. 1). It is likely that delivery of these cells via portal vein injection is relatively inefficient and that Kupffer cells may clear many transplanted cells,³⁰ but a proliferative cell that persists in the undamaged liver parenchyma is able to undergo more doublings than a less proliferative cell. This is supported by the observed increase in GFP+ cells retrieved from livers comparing 7 to 30 d posttransplant (Fig. 3A). Although we observed no teratoma or other tumor formation in the current study, a highly proliferative cell will need to be more fully vetted as unchecked proliferative activity can lead to DNA damage and tumorigenesis.³² Therefore, future experiments will examine this possibility using human stem cell derivatives transplanted into quiescent livers of rodent models.

Magnetic targeting to enhance aFGF-EP engraftment into the undamaged liver parenchyma has several advantages. First, magnetic targeting results in a higher proportion of transplanted cells in the liver immediately after delivery and up to 30 d postdelivery (Fig. 3A), indicating this strategy both increases the initial dwell time and the biomass ultimately generated by transplanted aFGF-EPs after 30 d. Second, based on a focused panel of gene expression measurements, magnetic targeting does not appear to negatively affect differentiation of aFGF-EPs *in vitro* (Fig. 2G) or

Fig. 3. (continued). and reported as percentages of total cells. Measurements of each time point represent an average of 3 mice with standard deviation (SD) shown with error bars (** $P < 0.01$, ns denotes not significant by two-way analysis of variance with Sidak's multiple comparisons test). (B) Representative stereo microscopy using FITC filter to analyze whole liver of mice 30 d after transplant as described in (A) without magnetic targeting (top, -magnet) and with magnetic targeting (bottom, +magnet) at 20 \times magnification. (C) Representative scatter plot showing FACS strategy to retrieve GFP+ cells from transplant recipient livers 30 d posttransplant. Signal overlay is shown to indicate auto versus true fluorescence: red represents a normal liver without cell transplant and green represents a liver 30 d after receiving GFP+ aFGF-EP transplant. Cells retrieved from quadrant 4 were used for analysis in (D) as GFP+ transplanted cells. (D) RNA was extracted, and liver-specific marker gene expression profiling was performed by RT-qPCR from SPM-labeled day 7 aFGF-EPs (day 7 SPM-EP), GFP+ cells retrieved from quadrant 4 in panel C (GFP+), native hepatocytes (hepatocytes), and spleen (spleen) with results shown normalized to β -actin and relative to day 7 EPs. ND represents undetectable expression; results are averages from 3 independent replicates with error bars shown as SD. (E) Representative fluorescent stereomicroscopy images from mouse liver (top) or lung (bottom) explant 7 d after receiving aFGF-EP cell transplant with (right; +SPM) or without (left; -SPM) magnetic targeting (5 \times magnification). (F) Average number of GFP+ cells detected per square millimeter field-of-view area using fluorescent microscopy (see E) to examine liver (left) or lung (right) explant, from mice 7 d after aFGF-EP transplant to the liver either with (+magnet) or without (-magnet) magnetic targeting. Results are reported as an average \pm SD of 3 mice; * $P < 0.05$ and ** $P < 0.01$ by Student's *t*-test.

in vivo (Fig. 3D), suggesting these hepatocyte-like cells could reverse a liver-based disease as we have previously demonstrated.¹⁴ Additionally, transplanted aFGF-EP cells may partially differentiate in vivo and form a population of liver stem cells capable of self-renewal and differentiation; however, further study is required to address this question. Third, we observe a significantly higher retention of transplanted cells in the liver versus the lung (Fig. 3E), suggesting a reduction in cellular pulmonary emboli that may be clinically significant. Also, since aFGF-EPs are much smaller than hepatocytes (cf. ~20 to ~40 μm), there is less risk of portal embolism. We do not observe overt evidence of portal stasis or inflammation in the current study either with or without magnetic targeting; however, additional studies are required to address these possibilities as well as determine how transplanted cells pass through the portal vasculature and presumably migrate through the space of Disse to ultimately colocalize with native hepatocytes. The sequence of events that results in long-term engraftment of EPs in the hepatocyte space is likely different from other cell types tested thus far but needs further delineation.

In conclusion, this approach represents an easily scalable, novel, and promising proof of concept that has the potential to translate directly to therapeutic strategies for specific liver-based genetic disorders.

Authors' Note

W. Samuel Fagg and Naiyou Liu contributed equally to this work.

Ethical Approval

This study was approved by our Institutional Animal Care and Use Committee (IACUC).

Statement of Human and Animal Rights

Animal procedures were approved by IACUC and monitored by institutional veterinary staff.

Statement of Informed Consent

There are no human subjects in this article and informed consent is not applicable.

Declaration of Conflicting Interests

The author(s) declared no potential conflicts of interest with respect to the research, authorship, and/or publication of this article.

Funding

The author(s) disclosed receipt of the following financial support for the research, authorship, and/or publication of this article: This work was supported in part by US National Institutes of Health, grant number HL082606-0 (Jeffrey Fair); the NIH National Institute of Diabetes and Digestive and Kidney Diseases, grant numbers DK079879 and DK090115 (Jae-Sung Kim); National Institute on Aging, grant number AG028740 (Jae-Sung Kim); and CIRM, grant number TG2-01157 (W. Samuel Fagg).

Supplemental Material

Supplementary material for this article is available online.

References

1. Cantz T, Sharma AD, Ott M. Concise review: cell therapies for hereditary metabolic liver diseases—concepts, clinical results, and future developments. *Stem Cells*. 2015;33(4):1055–1062.
2. Najimi M, Defresne F, Sokal EM. Concise review: updated advances and current challenges in cell therapy for inborn liver metabolic defects. *Stem Cells Transl Med*. 2016;5(8):1117–1125.
3. Stephenne X, Najimi M, Smets F, Reding R, de Ville de Goyet J, Sokal EM. Cryopreserved liver cell transplantation controls ornithine transcarbamylase deficient patient while awaiting liver transplantation. *Am J Transplant*. 2005;5(8):2058–2061.
4. Horslen SP, McCowan TC, Goertzen TC, Warkentin PI, Cai HB, Strom SC, Fox JJ. Isolated hepatocyte transplantation in an infant with a severe urea cycle disorder. *Pediatrics*. 2003;111(6 pt 1):1262–1267.
5. Asgari S, Moslem M, Bagheri-Lankarani K, Pournasr B, Miryounesi M, Baharvand H. Differentiation and transplantation of human induced pluripotent stem cell-derived hepatocyte-like cells. *Stem Cell Rev*. 2013;9(4):493–504.
6. Marongiu M, Serra MP, Contini A, Sini M, Strom SC, Laconi E, Marongiu F. Rat-derived amniotic epithelial cells differentiate into mature hepatocytes in vivo with no evidence of cell fusion. *Stem Cells Dev*. 2015;24(12):1429–1435.
7. Laconi E, Oren R, Mukhopadhyay DK, Hurston E, Laconi S, Pani P, Dabeva MD, Shafritz DA. Long-term, near-total liver replacement by transplantation of isolated hepatocytes in rats treated with retrorsine. *Am J Pathol*. 1998;153(1):319–329.
8. Puppi J, Strom SC, Hughes RD, Bansal S, Castell JV, Dagher I, Ellis EC, Nowak G, Ericzon BG, Fox JJ, et al. Improving the techniques for human hepatocyte transplantation: report from a consensus meeting in London. *Cell Transpl*. 2012;21(1):1–10.
9. Yamanouchi K, Zhou H, Roy-Chowdhury N, Macaluso F, Liu L, Yamamoto T, Yannam GR, Enke C, Solberg TD, Adelson AB, et al. Hepatic irradiation augments engraftment of donor cells following hepatocyte transplantation. *Hepatology*. 2009;49(1):258–267.
10. Khozouz RF, Huq SZ, Perry MC. Radiation-induced liver disease. *J Clin Oncol*. 2008;26(29):4844–4845.
11. Park W, Lim DH, Paik SW, Koh KC, Choi MS, Park CK, Yoo BC, Lee JE, Kang MK, Park YJ, et al. Local radiotherapy for patients with unresectable hepatocellular carcinoma. *Int J Radiat Oncol Biol Phys*. 2005;61(4):1143–1150.
12. Lee MT, Kim JJ, Dinniwell R, Brierley J, Lockwood G, Wong R, Cummings B, Ringash J, Tse RV, Knox JJ, et al. Phase I study of individualized stereotactic body radiotherapy of liver metastases. *J Clin Oncol*. 2009;27(10):1585–1591.
13. Fair JH, Cairns BA, Lapaglia MA, Caballero M, Pleasant WA, Hatada S, Kim HS, Gui T, Pevny L, Meyer AA, et al. Correction of factor IX deficiency in mice by embryonic stem cells differentiated in vitro. *Proc Natl Acad Sci U S A*. 2005;102(8):2958–2963.
14. Fair JH, Cairns BA, Lapaglia M, Wang J, Meyer AA, Kim H, Hatada S, Smithies O, Pevny L. Induction of hepatic differentiation in embryonic stem cells by co-culture with embryonic cardiac mesoderm. *Surgery*. 2003;134(2):189–196.

15. Kubo A, Shinozaki K, Shannon JM, Kouskoff V, Kennedy M, Woo S, Fehling HJ, Keller G. Development of definitive endoderm from embryonic stem cells in culture. *Development*. 2004;131(7):1651–1662.
16. Strober W. Trypan blue exclusion test of cell viability. *Curr Protoc Immunol*. 2001; Appendixes 3, 3B. doi: 10.1002/0471142735.ima03bs21.
17. Kim JS, He L, Qian T, Lemasters JJ. Role of the mitochondrial permeability transition in apoptotic and necrotic death after ischemia/reperfusion injury to hepatocytes. *Curr Mol Med*. 2003;3(6):527–535.
18. Tajbakhsh J, Gertych A, Fagg WS, Hatada S, Fair JH. Early in vitro differentiation of mouse definitive endoderm is not correlated with progressive maturation of nuclear DNA methylation patterns. *PLoS One*. 2011;6(7):e21861.
19. Tajbakhsh J, Stefanovski D, Tang G, Wawrowsky K, Liu N, Fair JH. Dynamic heterogeneity of DNA methylation and hydroxymethylation in embryonic stem cell populations captured by single-cell 3D high-content analysis. *Exp Cell Res*. 2015;332(2):190–201.
20. Caballero M, Lightfoot HM Jr, Lapaglia M, Pleasant A, Hatada S, Cairns BA, Fair JH. Detection and characterization of hepatic engraftment of embryonic stem derived cells by fluorescent stereomicroscopy. *J Surg Res*. 2007;141(2):134–140.
21. Cheng K, Li TS, Malliaras K, Davis DR, Zhang Y, Marbán E. Magnetic targeting enhances engraftment and functional benefit of iron-labeled cardiosphere-derived cells in myocardial infarction. *Circ Res*. 2010;106(10):1570–1581.
22. Vanecek V, Zablotskii V, Forostyak S, Růžička J, Herynek V, Babič M, Jendelová P, Kubinová S, Dejneka A, Syková E. Highly efficient magnetic targeting of mesenchymal stem cells in spinal cord injury. *Int J Nanomedicine*. 2012;7:3719–3730.
23. Kamei G, Kobayashi T, Ohkawa S, Kongcharoensombat W, Adachi N, Takazawa K, Shibuya H, Deie M, Hattori K, Goldberg JL, et al. Articular cartilage repair with magnetic mesenchymal stem cells. *Am J Sports Med*. 2013;41(6):1255–1264.
24. Zhao S, Wang Y, Gao C, Zhang J, Bao H, Wang Z, Gong P. Superparamagnetic iron oxide magnetic nanomaterial-labeled bone marrow mesenchymal stem cells for rat liver repair after hepatectomy. *J Surg Res*. 2014;191(2):290–301.
25. Wilhelm C, Billotey C, Roger J, Pons JN, Bacri JC, Gazeau F. Intracellular uptake of anionic superparamagnetic nanoparticles as a function of their surface coating. *Biomaterials*. 2003;24(6):1001–1011.
26. Gupta S, Rajvanshi P, Sokhi R, Slehria S, Yam A, Kerr A, Novikoff PM. Entry and integration of transplanted hepatocytes in rat liver plates occur by disruption of hepatic sinusoidal endothelium. *Hepatology*. 1999;29(2):509–519.
27. Baccarani U, Adani GL, Sanna A, Avellini C, Sainz-Barriga M, Lorenzin D, Montanaro D, Gasparini D, Risaliti A, Donini A, et al. Portal vein thrombosis after intraportal hepatocytes transplantation in a liver transplant recipient. *Transpl Int*. 2005;18(6):750–754.
28. Weber A, Groyer-Picard MT, Franco D, Dagher I. Hepatocyte transplantation in animal models. *Liver Transpl*. 2009;15(1):7–14.
29. Guo D, Fu T, Nelson JA, Superina RA, Soriano HE. Liver repopulation after cell transplantation in mice treated with retorsine and carbon tetrachloride. *Transplantation*. 2002;73(11):1818–1824.
30. Joseph B, Malhi H, Bhargava KK, Palestro CJ, McCuskey RS, Gupta S. Kupffer cells participate in early clearance of syngeneic hepatocytes transplanted in the rat liver. *Gastroenterology*. 2002;123(5):1677–1685.
31. Puppi J, Tan N, Mitry RR, Hughes RD, Lehec S, Mieli-Vergani G, Karani J, Champion MP, Heaton N, Mohamed R, et al. Hepatocyte transplantation followed by auxiliary liver transplantation—a novel treatment for ornithine transcarbamylase deficiency. *Am J Transplant*. 2008;8(2):452–457.
32. Evan GI, Vousden KH. Proliferation, cell cycle and apoptosis in cancer. *Nature*. 2001;411(6835):342–348.